Transcriptional response of the calcification and stress response toolkits in an octocoral under heat and pH stress

Sergio Vargas[1,*], Thorsten Zimmer[1], Nicola Conci[1], Martin Lehmann[2], Gert Wörheide[1,3,4]

Author affiliations:

1. Department of Earth and Environmental Sciences, Paleontology & Geobiology, Ludwig-Maximilians-Universität München, Richard-Wagner-Str. 10, 80333 München, Germany.
2. Biozentrum der LMU München, Department of Biology I–Botany, Grosshaderner Strasse 2–4, Planegg-Martinsried, Germany.
3. GeoBio-Center, Ludwig-Maximilians-Universität München, Richard-Wagner-Str. 10, 80333 München, Germany.
4. SNSB – Bayerische Staatssammlung für Paläontologie und Geologie, Richard-Wagner-Str. 10, 80333 München, Germany.

* Corresponding author: sergio.vargas@lmu.de

Abstract

Up to one-third of all described marine species inhabit coral reefs, but the future of these hyperdiverse ecosystems is insecure due to local and global threats, such as overfishing, eutrophication, ocean warming, and acidification. Although these impacts are expected to have a net detrimental effect on reefs, it has been shown that some organisms like octocorals may remain unaffected, or benefit from, anthropogenically induced environmental change, and may replace stony corals in future reefs. Despite their potential importance in future shallow-water coastal environments, the molecular mechanisms leading to the resilience to anthropogenic-induced stress observed in octocorals remain unknown. Here, we use manipulative experiments,

proteomics, and transcriptomics to show that the molecular toolkit used by *Pinnigorgia flava*, a common Indo-Pacific gorgonian octocoral, to deposit its calcium-carbonate skeleton is resilient to heat and seawater acidification stress. Sublethal heat stress triggered a stress response in *P. flava* but did not affect the expression of 27 transcripts encoding Skeletal Organic Matrix (SOM) proteins. Exposure to seawater acidification did not cause a stress response but triggered the downregulation of many transcripts, including an osteonidogen homolog present in the SOM. The observed transcriptional decoupling of the skeletogenic and stress-response toolkits provides insights into the mechanisms of resilience to anthropogenically-driven environmental change observed in octocorals.

Keywords: Biomineralization, Calcification, Climate change, Cnidaria, Octocorals, Resilience.

Introduction

As a consequence of anthropogenic-induced global climate change, extreme climatic events, like the heat waves affecting the Great Barrier Reef in 2016, 2017, and 2020, are likely to increase in frequency, impacting marine communities in unprecedented ways (Hughes et al., 2017, 2018, 2019). In coral reefs, these phenomena can lead to the displacement of stony corals as the dominant reef-building taxon by other benthic organisms and can cause community phase shifts with ecosystem-level effects (Done, 1992). Both theoretical (Fung, Seymour, & Johnson, 2011) and empirical (Schmitt, Holbrook, Davis, Brooks, & Adam, 2019) studies predict and support coral reef phase shifts leading to the dominance of diverse groups, including algae, sponges, and other cnidarians such as corallimorpharians and octocorals in these ecosystems (see Norström, Nyström, Lokrantz, & Folke, 2009 for a review).

Octocorals (e.g., soft-corals, gorgonians) are common and important community members in many marine ecosystems. They increase the spatial complexity of the habitats they inhabit (Quattrini et al.,

2014) and provide refuge to numerous invertebrate species (Buhl-Mortensen & Mortensen, 2005; Cúrdia et al., 2015). In shallow water ecosystems, such as coral reefs, octocorals can outgrow stony corals and become dominant after extreme climatic events, like anomalously strong El Niño events (Ruzicka et al., 2013), or under extreme environmental conditions, like those prevailing in volcanic-seep acidified waters (Inoue, Kayanne, Yamamoto, & Kurihara, 2013). For instance, in Florida, octocorals increased in abundance in the 11 years following the 1997/98 El Niño event, becoming the most abundant taxon in some localities and dominating shallow fore-reefs (Ruzicka et al., 2013). Similarly, the soft coral genus *Rhytisma* became dominant after a significant coral bleaching event in the Aldabra Atoll (Indian ocean) in 1998 (Spencer et al., 2005), and the "blue coral," *Heliopora coerulea*, a species of the reef-building zooxanthellate octocoral clade Helioporacea, increased its abundance to > 50% over a decade in the Bolinao Reef Complex in the northern Philippines (Atrigenio, Aliño, & Conaco, 2017). Like scleractinians, helioporacean octocorals produce a rigid skeleton made of aragonite (a polymorph of calcium carbonate) (Colgan, 1984), but their calcification machinery appears to be more resilient to environmental stressors than that of most scleractinians (Kayanne, Harii, Ide, & Akimoto, 2002; Shaish, Levy, Katzir, & Rinkevich, 2010). Thus, octocorals may be possible winners in future oceans due to global climate change, potentially replacing scleractinians as the main reef framework-building organisms (Inoue et al., 2013).

Studies on scleractinian corals indicate that these organisms' response to anthropogenic-driven climate change depends on the stress source and differs among species and ontogenetic stages (Davies, Marchetti, Ries, & Castillo, 2016; Moya et al., 2012; Thomas et al., 2018). In *Acropora hyacinthus*, heat stress triggers a large and dynamic transcriptomic response characterized by the modulation of different metabolic and cell cycle processes in the early stress response and of spliceosome activity, RNA- and DNA-related metabolic processes, cell stress, and cell metabolism before bleaching onset (Seneca & Palumbi, 2015). A meta-analysis of the transcriptomic response to different stress sources in ten *Acropora* species identified an "environmental stress response" toolkit consisting of genes involved in the response to reactive oxygen species, protein folding and

degradation, NF-κB signaling, immune response, and cell death (Dixon, Abbott, & Matz, 2020) that corals exposed to environmental stress consistently modulated. In contrast, ocean acidification does not appear to trigger a pronounced transcriptional response in adult corals colonies (Davies et al., 2016; González-Pech, Vargas, Francis, & Wörheide, 2017) but elicit the modulation of several calcification-related genes in the primary polyps of *Acropora millepora* (Moya et al., 2012).

Despite the observed higher tolerance of octocorals to climate change-induced stress, their physiological response to these stimuli remains poorly studied. Wiens et al. (2000) and Shimpi et al. (2016) observed Heat-Shock Protein overexpression in thermally stressed *Dendronephthya klunzingeri* and *Sinularia* cf. *cruciata* colonies, respectively. Similarly, the sea pen *Veretillum cynomorium* displayed elevated heat-shock protein concentrations upon exposure to thermal stress, but this species did not show increased antioxidant or lipid peroxidation activities (Lopes et al., 2018). To date, aside from these limited data on the octocoral response to environmental stress, no assessment of the transcriptomic response of octocorals exist, and the resilience mechanisms used by these organisms to tolerate and, eventually, outgrow and outcompete less resilient organisms, like stony corals, remain largely unknown.

However, since growth in octocorals requires the deposition of new calcium-carbonate skeletal elements (calcite sclerites, or aragonite fibers in case of the blue corals) to support the colony structurally (Lewis & Vonwallis, 1991), resilience to climate change in this group must be linked to their ability to sustain calcification under challenging environmental conditions (Gabay, Benayahu, & Fine, 2013; Gabay, Fine, Barkay, & Benayahu, 2014; Gómez et al., 2015; Inoue et al., 2013). Indeed, except for the Helioporacea, the octocoral tissues effectively isolate sclerocytes from the surrounding seawater (Gabay et al., 2014), putatively allowing these cells to sustain the expression of transcripts involved in calcification under situations of environmental stress, and the colonies to outgrow and outcompete less resilient organisms. To test this hypothesis, we characterized the skeletal proteome of the common Indo-Pacific gorgonian octocoral *Pinnigorgia flava* and used

manipulative experiments and transcriptomics to assess the effect of heat and pH stress on the expression of transcripts involved in calcification in this species. Together, our data provide a first assessment of the transcriptional response an octocoral to environmental stress factors induced by anthropogenically driven climate change and gives insights into the octocoral resilience mechanisms.

Materials and Methods

Experimental model and subject details

We used clonal explants of a colony of *Pinnigorgia flava* (Nutting, 1910) kept at 25 °C and a 12:12 h light cycle in a 642 L marine aquarium system at the Department of Earth- and Environmental Sciences, Paleontology and Geobiology, Ludwig-Maximilians Universität München (see below). *Pinnigorgia flava* is a colonial, zooxanthellate soft coral (Octocorallia) largely endemic to the Great Barrier Reef but sporadically found in the coral triangle in SE Asia. The studied colony is cultured in our research aquaria for more than a decade, its exact geographic origin is unknown. It forms non-anastomosing, pinnated light purple colonies with brownish polyps. The sclerites are white to yellow bent spindles, capstans, and rods. Currently, *P. flava* belongs to the family Gorgoniidae.

Determination of calcification hotspots along the body axis of P. flava

We used calcein, a calcium-binding fluorescent dye that permanently incorporates into newly formed skeleton, to investigate the distribution of calcification sites along the body axis of *P. flava* (Holcomb, Cohen, & McCorkle, 2013/2). We incubated three colonies of *P. flava* for 72 h in a glass container with 500ml of a 50µg/ml calcein disodium salt (Sigma-Aldrich) in 0.2 µm filtered artificial seawater (Suppl. Fig. 1). We exchanged the seawater with fresh seawater+calcein every 24 h. After staining, we fixed the colonies in 80% EtOH and stored them at ~5 °C until further processing.

To assess whether calcification preferentially occurs on the tip of the colonies or, on the contrary, the calcification hotspots occur along the colony body axis, we cut the colonies in top and bottom sections using a sterile scalpel and placed each piece in 1.5 ml microcentrifuge tubes containing one ml of sodium hypochlorite (NaOCl 10%; Fluka). After a three-hour bleach incubation, we rinsed the sedimented sclerites six times with distilled water and stored them in 80% ethanol. We then placed a sample of sclerites onto glass slides and embedded them in Eukitt quick-hardening mounting medium (Fluka Analytical) before covering the sample with a glass coverslip.

We observed the sclerites under epifluorescence (excitation band-pass filter 420-490 nm, barrier long-pass filter 515 nm) on a Leica DMLB microscope coupled to a Leica DFC 480 camera and an I3 filter set. We exposed the stained sclerites for ten seconds and acquired pictures using Leica Application Software "LAS V4.5". To determine the number of stained sclerites per colony region, we sampled the top and bottom fragments of the colonies and counted stained and total sclerites per visual field at a 100X magnification along one horizontal transect crossing the slide from left to right.

Proteomic analysis of the skeletal organic matrix of P. flava's *sclerites*

To determine the skeletal proteome of *P. flava*, we sampled four colonies of about four centimeters in length and incubated them in sodium hypochlorite (5%, Fluka) for 72 h under moderate shaking (30 rpm; IKA Rocker 3D digital). We then rinsed the sedimented sclerites six times with Milli-Q water and dried them at 37°C for 24 h. This procedure yielded approximately 0.75 g of dry sclerites, which we ground with a mortar and pestle before incubating again in sodium hypochlorite (2%) for four hours under moderate mixing (30 rpm). After bleaching, we rinsed the powder six times with Milli-Q water and dried it overnight at 37°C. To dissolve the calcitic mineral, we incubated the dry powder in 10% acetic acid overnight under moderate mixing (20 rpm). We centrifuged the resulting solution at

155 13,500 rpm for 30 min to separate the acetic-insoluble matrix (AIM) from the acetic-soluble matrix
156 (ASM). To isolate the ASM, we centrifuged (4600 rpm for 70 min at 16°C) the supernatant through
157 15 mL Amicon ultrafiltration devices with a 3 kDa cutoff membrane and added four volumes of
158 methanol, one volume of chloroform, and three volumes of Milli-Q water to one volume of desalted
159 solution to precipitate the proteins by centrifugation at 5,500 rpm for 15 min (Wessel & Flügge,
160 1984). After discarding the upper phase, adding three volumes of methanol, and centrifuging the
161 sample at 5,500 rpm for 15 min, we air-dried the resulting ASM pellet and resuspended both the
162 ASM and AIM fractions in 95% Laemmli buffer + 5% β-mercaptoethanol. We used a 1-dimensional
163 sodium dodecyl sulfate-polyacrylamide (SDS-PAGE) gel (Mini-PROTEAN Tetra System, Bio-Rad, USA)
164 to separate electrophoretically the skeletal organic matrix proteins before mass spectrometry. To
165 visualize the extracted SOM protein fractions, we ran an SDS-PAGE for 90 min at 80V, increasing the
166 voltage to 100V after the gel front passed the boundary between the stacking and the resolving gel.
167 We used the Precision Plus Protein Dual Xtra Standard (Bio-Rad, 12 band marker, 2kD-250kD) as a
168 size standard and stained the gel after fixing for 20 min in a fixation solution (50% ethanol, 40% Milli-
169 Q, and 10% acetic acid), washing in 30% ethanol for ten minutes, and in Milli-Q water for ten
170 minutes, with silver nitrate using the Proteo Silver Plus Silver Stain Kit (Sigma-Aldrich, USA). For this,
171 we incubated the gel in sensitizer solution for ten minutes, washed it as described above, and
172 equilibrated it for ten minutes in the silver solution. Before developing, we washed the stained gel
173 for one minute in Milli-Q water and submerged it in a developing solution for five minutes. After
174 stopping the development reaction, we washed the gel for 15 min in Milli-Q water. We used an
175 orbital shaker at 60 rpm for all steps described above. For mass spectrometry, we ran the SDS-PAGE
176 with the six technical replicates of the extracted SOM protein fractions for 40 min at 80V until the
177 protein extracts passed the boundary between the stacking and the resolving gel, and manually
178 excised the bands with a sterile scalpel. We then subjected the isolated proteins to alkylation,
179 reduction, and tryptic digestion (0.1 µg/µl trypsin at 37°C, overnight). We used an LTQ Orbitrap mass
180 spectrometer (Thermo Fisher Scientific, Waltham, Massachusetts, USA) coupled with a Rheos Allegro

181 liquid chromatograph (Flux Instruments GmbH, Basel, Switzerland) to analyze three µl of the
182 digested sample after separation using a self-made column of 75 µm diameter, 15 cm length, C18
183 particles of 2 µm diameter and 100 Å pore size (Dr. Maisch GmbH, Ammerbruch-Entringen,
184 Germany). We prepared the MS grade mobile phases as follows A) water containing 10% acetonitrile
185 (ACN), B) ACN containing 10% water, each combined with 0.1% formic acid. We used the following
186 gradient: 40 min (0-23% B), 40 min (23-85% B), five minutes (85-100% B), 25 min (100% B), three
187 minutes (100-0% B) and 20 min (0 % B) for re-equilibration, and a constant 40 µl/min flow at RT
188 (22°C). We used the programs Xcalibur 2.0 (Thermo Fisher Scientific Inc., 30 Waltham, USA) and
189 MaxQuant Version 1.5.2.8 (Cox andf Mann 2008, doi: 10.1038/nbt.1511) to acquire and analyze the
190 MS/MS data, respectively. We estimated protein abundances as relative iBAQ values
191 (Schwanhäusser et al., 2011) of the detected SOM proteins using the MaxLFQ algorithm (Cox et al.,
192 2014). We filtered the LC-MS/MS results to remove hits from known conventional contamination
193 sources using the common Repository Adventitious Proteins (cRAP) database before mapping the
194 peptides against a transcriptome reference of *P. flava* (Conci, Wörheide, & Vargas, 2019). We
195 translated the transcripts matching proteins present in the SOM fractions and annotated them
196 against the UniProtKB database using blastp (https://blast.ncbi.nlm.nih.gov/) and SignalP 4.0
197 (Petersen, Brunak, von Heijne, & Nielsen, 2011) to predict the presence of signal peptides,
198 transmembrane regions, and GPI anchors within the predicted protein sequences. Additionally, to
199 assess the distribution of the detected *P. flava* SOM proteins among cnidarians, we screened a
200 database composed of 120 transcriptomes from representatives of this phylum using *P. flava's* SOM
201 proteins as queries for the search (for details see Eitel et al., 2018).
202
203 *In vivo experiments:*
204
205 We used a 360 L marine aquarium under a 12:12 h light cycle controlled by GHL Mitras LX 6200-HV
206 LED lights that yielded ten kLux (PAR = 250 µmol/m^{2}s) at the water surface. Based on hourly

measurements over one year (2017), the system's average water temperature and pH are 24.92 ± 0.24 °C and 8.30 ± 0.14, respectively. Based on weekly measurements over one year (2017), the average PO_4^{-3}, NO_2^- and NO_3^- concentrations in the water are 0.092 ± 0.071 mg/L, 0.014 ± 0.072 mg/L, 2.681 ± 3.882 mg/L; the concentration of NH_3/NH_4^+ in the water was consistently below detection (i.e. < 0.05 mg/L). Weekly or daily monitoring in subsequent years revealed that these values are stable and can be taken as a baseline for the system. We measured the PO_4^{-3}, NO_2^-, NO_3^- and NH_3/NH_4^+ concentrations every other day during the experiments. The measured concentrations did not differ from the baseline concentrations for the tank.

To assess the effect of heat stress on *P. flava*, we randomly assigned nubbins (n = 18) to six aquaria (10L) filled with approximately six liters of artificial seawater and partially immersed in the 360 L aquarium described above. Water evaporation in the ten-liter tanks was compensated every day with water filtered by reverse osmosis. We used a submersible water pump (300 L/h; Eheim, Germany) to provide adequate water mixing in each tank. For the temperature experiment, after an acclimation period of four days, we randomly selected three tanks and gradually increased the water temperature to 29-30°C for five days (~1°C per day) using 50 W water heaters (Eheim, Deizisau, Germany). We then kept the *P. flava* colonies at 29-30°C for three days. Although the bleaching threshold of *P. flava* is not known, considering that the colony used for our experiments grows since >ten years at a 25 °C, the final water temperature (i.e., 29-30°C) achieved during the experiment lies >four °C over the mean water temperature this coral is exposed to. Thus, the increase in temperature from 25°C to 29-30°C is expected to cause a heat stress response in *P. flava* without necessarily causing its death. In scleractinian corals, for example, bleaching can be induced by heat stress only about 1°C above the average summer maximum temperature. During the experimental period, we monitored water pH, density, and temperature (manually twice per day) every day (Suppl. Tables 1-3). We also measured the nutrient profile in the ten-liter tanks at the end of the experiment. The observed physicochemical values were similar to those of the main tank, and most

nutrients were below the detection limit of the tests used. We also visually monitored the colonies, which had their polyps everted and did not show any visible signs of bleaching during the experiment. In this regard, the bleaching threshold is not known for *P. flava*. At the end of the experiment, we cut octocorals in two (i.e., lower and upper) sections using sterile scissors and flash-froze them in liquid nitrogen before storing them at -80°C until further processing.

We assessed the effect of seawater acidification on twelve colonies of *P. flava* distributed in two 30 L tanks (control and treatment) connected to a 320 L salt-water "mother" tank. To lower (0.1 pH units drop per day) the seawater pH, we pumped CO_2 into the treatment tank (see details in González-Pech et al., 2017) to achieve a pH of 7.8 (from a starting value of 8.2). We kept the pH stable for three days and lowered it again to 7.6 over three days. After reaching pH = 7.6, we allowed the octocorals to acclimate for three days before decreasing the pH to its final value of 7.3. Gomez et al. (2015) showed that *Eunicea fusca* grows under a broad range of seawater pH values but possibly experience some level of decalcification at pH = 7.1. Therefore, we used a pH = 7.3 to evaluate *P. flava*'s response to seawater acidification as this value represents the lowest reported pH value at which octocorals continue growing without sclerite decalcification. We maintained this pH for two months using an automatic pH computer and monitored it throughout the experiment using a PCE-PHD 1 datalogger (PCE Instruments, Germany). The pH of the "mother" and control tank was 8.2 throughout the experiment. The temperature and nutrient levels in the "mother" tank were as detailed above. During the entire experimental phase, the coral colonies showed everted polyps and no signs of stress (e.g., bleaching). At the end of the experiment, we cut the octocorals at the base using sterile scalpels and then flash-froze them in liquid nitrogen before storing them at -80°C until further processing.

Analysis of differential gene expression

259 We extracted total RNA from the upper section of the octocorals using the Direct-zol RNA MiniPrep
260 kit (Zymo Research) following the manufacturer's protocol. We assessed the purity and integrity of
261 the RNA extracts using a Nanodrop ND-1000 spectrophotometer (Thermo Fisher Scientific, USA) and
262 a Bioanalyzer 2100 (Agilent Inc., USA). In general, all samples showed 260/230 and 260/280 ratios >
263 2.0 and RIN values above 8.5. We used Lexogen's SENSE Total RNA-Seq Library Prep Kit according to
264 the manufacturer's instructions to generate Illumina-ready, stranded transcriptome libraries for all
265 extracted samples. We sequenced the libraries (50bp Pair-End) in an Illumina HiSeq2000 (see Suppl.
266 Table 4), discarded reads with an average quality < Q28, stretches of poly-{ATCG} or Illumina
267 adapters using the program *bl-filter-illumina* from the BioLite suite (Howison, Sinnott-Armstrong, &
268 Dunn, 2012), and mapped them to an available *P. flava* holobiont reference transcriptome (Conci et
269 al., 2019) using Salmon (Patro, Duggal, Love, Irizarry, & Kingsford, 2017). We truncated the resulting
270 (holobiont) pseudocounts matrix and analyzed it using DESeq2 (Love, Huber, & Anders, 2014) to
271 determine differentially expressed genes (DGE) in 1) control vs. heat stress treated and 2) control vs.
272 pH stress treated octocorals. For each stress treatment (i.e., temperature and pH stress) we
273 separated host and symbiont DGEs in R using lists of host and symbiont transcripts determined using
274 PsyTrans (REFS). We used the obtained list of host DEGs for GO-term enrichment analyses with
275 TopGO (Alexa & Rahnenfuhrer, 2016) using a Fisher test on nodes with at least five annotations. To
276 summarize the resulting list of significantly enriched GO-terms, we used the R package GOSemSim
277 (Yu et al., 2010) to calculated the pairwise semantic similarity (Wang) between GO-terms and
278 clustered (Ward) the enriched GO-terms into groups of semantically related GO-terms. To assign a
279 representative GO-term to each cluster of semantically related, significantly enriched GO-terms in
280 the different stress treatments, we took advantage of the hierarchical structure of the gene ontology
281 and retrieved subgraphs including the GO-terms in each cluster. These subgraphs show how
282 semantically similar GO-terms relate to each other in the more broad gene ontology directed acyclic
283 graph. We used these subgraphs graphs to find GO-terms from which other GO-terms in a cluster
284 derived (i.e., "ancestor" GO-terms) and used these more general GO-terms as cluster descriptors.

285

286 **Results**

287

288 *Calcification in* P. flava *occurs along its entire body axis*

289

290 Visual inspection of stained sclerites in the top vs. bottom parts of *P. flava* colonies revealed that this
291 species produces new sclerites in both the top and bottom sections of the colony, with a slight but
292 significant increase in the proportion of stained sclerites toward the tips of the colony (Welch two-
293 sample t=-2.17, df=92.531, p=0.034). Examination of whole colonies sections revealed that
294 calcification usually occurs at the polyps (Fig. 1). Despite the increased number of stained sclerites at
295 the colony's top, we could not detect any evident calcification hotspots along the colony axis.

296

297 *Taxonomically widespread and restricted proteins form the skeletal proteome of* P. flava

298

299 After filtering potential known contaminants (e.g., keratins, trypsin), we identified a total of 27
300 transcripts as the skeletal organic matrix (SOM) proteome of *P. flava*. Label-free quantification (LFQ)
301 revealed 14 proteins with a higher abundance in the acetic-insoluble matrix (AIM), seven proteins
302 exclusive to the acetic-soluble matrix (ASM), and five proteins shared by both fractions (Fig. 2).
303 Biochemically, seven of the detected SOM proteins are membrane-bound, containing either
304 transmembrane domains (n = 3), GPI anchors (n = 3), or both (n = 1). About 46% (n = 13) of the SOM
305 proteins detected contain signal peptide motifs, indicating that these proteins are secretion targets
306 (Fig. 2). We found the SOM proteome to contain several components of the extracellular matrix.
307 Among them are collagens and laminin, glycoproteins with calcium-binding domains (i.e.,
308 osteonidogen and agrin), and proteins likely involved in cell adhesion (i.e., otoancorin, hemicentin,
309 and von Willebrand factor type A (VWA) domain bearing proteins). Finally, we found a protein
310 similar to galaxin, two proteins enriched in aspartic-acid residues (acidic, predicted pI ~ 3.4) with no

311 significant UniProt blast hits, and several other proteins with diverse functionalities (e.g., disulfide
312 isomerase or protease activity). According to their iBAQ, six proteins had abundances >5% in the
313 skeletal proteome of *P. flava*. The two acidic proteins ranked first and third, osteonidogen and
314 collagen were the second and fourth most abundant proteins, and galaxin and agrin ranked fifth and
315 sixth in abundance. These six proteins account for 90% of the total iBAQ-derived skeletal protein
316 abundance (Fig. 2). On average, the remaining proteins accounted for only 0.5% (±0.6%) of the total
317 iBAQ-derived abundance.
318
319 In terms of their taxonomic distribution within Cnidaria (Fig. 2), similarity searches revealed that the
320 skeletal proteome of *P. flava* includes proteins with a widespread distribution in this group, such as
321 all detected collagens, agrin, osteonidogen, galaxin, and several enzymes, among others. Other
322 proteins, like hemicentin or the protein kinase Nell 1, displayed a patchier occupancy and were
323 found mostly in other anthozoans. Finally, only a few SOM components, namely the two acidic
324 proteins found, a serine protein-kinase receptor and a protein similar to laminin, had a restricted
325 taxon occupancy with significantly similar proteins found almost exclusively in other octocorals (i.e.,
326 Order Alcyonacea).
327
328 *Climate change-driven stress does not modulate the calcification toolkit of* P. flava
329
330 Exposure to sublethal, high-temperature (~29-30°C, ~5°C above long-term average in the aquaria)
331 seawater resulted in the modulation of 751 host transcripts (Benjamini-Hochberg corrected $p <$
332 0.05), 108 transcripts upregulated (log2 fold change ≥ 1) and with 221 transcripts downregulated
333 (log2 fold change ≤ -1) in heat-treated colonies (Fig. 3A, Suppl. Fig. 2, and Suppl. Table 5). We found
334 two representatives of the heat-shock protein 70 family among the transcripts upregulated by heat
335 stress (Fig. 3B). Among calcification-related proteins, heat stress caused the downregulation of one
336 carbonic anhydrase and one galaxin, not affecting the remaining 25 calcification-related proteins

337 previously identified in octocorals (Conci et al., 2019). Also, heat stress did not significantly change
338 the expression of any of the 27 transcripts encoding SOM proteins in *P. flava* (Fig. 3B).
339
340 The GO-term enrichment analysis of the set of upregulated transcripts during heat stress resulted in
341 seven clusters of semantically similar, significantly enriched Biological Process (BP) GO-terms (Fig. 4
342 and Suppl. Fig. 3-16). The representative GO-terms of these clusters were related to processes of
343 "programmed cell death" (GO:0012501) and the "regulation of apoptotic processes" (GO:0042981),
344 "response to stress" (GO:0006950) and "adaptive immune responses" (GO:0002250), protein folding
345 (several GO-terms, see S. Materials), redox and metabolic processes, peptide secretion and
346 epidermis development. Detailed information about the GO-terms included in each cluster, the
347 values of the Fisher-test, and the information content of each GO-term in the clusters is provided in
348 the Suppl. Tables 6-12. We found seven clusters of semantically similar, significantly enriched BP GO-
349 terms among transcripts downregulated by heat stress (Fig. 5 and Suppl. Fig. 17-30). These clusters
350 were related to the "cellular response to (increased) oxygen levels" (GO:0071453), the "regulation of
351 cellular response to oxidative stress" (GO:1900407), "cartilage development" (GO:0051216),
352 including terms related to bone morphogenesis, "immune response" (GO: 0006955), the "regulation
353 of necrotic death" (GO:0010939), and more miscellaneous GO-terms such as fatty acid elongation
354 (GO:0019367 and GO:0019368) and secondary metabolic processes. Detailed information about the
355 GO-terms included in each cluster, the values of the Fisher-test, and the information content of each
356 GO-term in the clusters is provided in the Suppl. Tables 13-19.
357
358 In contrast to the response of the coral, heat stress resulted in the modulation of only 19 transcripts
359 in *P. flava*'s symbionts; nine of these transcripts had a log2 fold change ≥ 1 and only one transcript
360 had log2 fold change ≤ -1 (Suppl. Table 20).
361
362 Contrary to heat stress, pH stress did not trigger a stark stress response in *P. flava,* only causing the

363 significant ($p < 0.05$) downregulation of a set of 70 host transcripts, 61 of which had a log2 fold
364 change ≤ -1 (Fig. 6A, Suppl. Fig. 31, and Suppl. Table 21). We found one calcification-related,
365 uncharacterized skeletal matrix protein and two SOM-encoding transcripts, namely osteonidogen --
366 the second more abundant SOM protein-- and a prosaposin-homolog downregulated in pH stressed
367 corals (Fig. 6B). We did not detect changes in the expression of stress-related proteins from the
368 Heat-Shock Protein family (Fig. 6B). Our GO-term enrichment analysis resulted in nine clusters of
369 semantically similar, significantly enriched BP GO-terms (Fig. 7 and Suppl. Fig. 32-49). These clusters
370 were related to the "regulation of metalloendopeptidase activity" (GO:1904683), "protein
371 localization to synapse" (GO:0035418), "regulation of bone mineralization" (GO:0030500) and
372 "regulation of biomineral tissue development" (GO:0070167), "terpenoid metabolic process"
373 (GO:0006721), "interaction with host" (GO:0051701), "response to BMP" (GO:0071772) and
374 "transmembrane receptor protein serine/threonine kinase signaling pathway" (GO:0007178),
375 "regulation of leucocyte proliferation" (GO:0070663) and "adaptive immune response"
376 (GO:0002250). We found one cluster grouping largely unrelated GO terms difficult to summarize
377 with a single representative GO term. Detailed information about the GO-terms included in each
378 cluster, the values of the Fisher-test, and the information content of each GO-term in the clusters is
379 provided in the Suppl. Tables 22-30.
380
381 pH stress did not result in the upregulation of any transcript in *P. flava* or the modulation of any
382 transcripts in *P. flava*'s symbionts.

383 **Discussion**

384 Sclerite growth in octocorals involves the synthesis by sclerocytes of skeletal organic matrix (SOM)
385 proteins and their transport to a sclerite-forming vacuole where primordia, mostly made of
386 irregularly shaped $CaCO_3$ crystals, form (Kingsley, 1984). Sclerite primordia continue growing by the
387 deposition of more regular crystals in an extracellular space created by multiple sclerocytes

388 (Goldberg & Benayahu, 1987). In *P. flava*, our results indicate that the deposition of new sclerites
389 occurs throughout the colony axis, increasing toward the colony tips. This pattern of calcification is
390 similar to that of *Leptogorgia virgulata*, one of the few other octocoral species where data on
391 calcification dynamics exist (Kingsley & Watabe, 1989). It indicates that active sclerocytes intersperse
392 along the colony axis and that under normal conditions, we should not expect spatial differences in
393 the expression of SOM-encoding transcripts in this species. Hence, the exposure of colonies of *P.*
394 *flava* to stress factors affecting the expression of SOM encoding transcripts should impair the
395 deposition of new sclerites at the colony level. The collapse of the calcification machinery, in turn,
396 would result in a reduced ability of octocorals to sustain growth and eventually outcompete other
397 reef organisms, like stony corals, in stressful environments.
398
399 The skeletal proteome of *P. flava* is similar to previously characterized proteomes in octo- and
400 scleractinian corals (Conci, Lehmann, Vargas, & Wörheide, 2020; Drake et al., 2013; Ramos-Silva et
401 al., 2013) and contains a mixture of taxonomically restricted and widespread elements as reported in
402 other octocorals (Conci et al., 2020). This trend is particularly evident among the most abundant
403 proteins in the SOM. Among those, galaxin and the two acidic proteins detected had a very narrow
404 taxonomic distribution. Galaxins mainly occur within Cnidaria (Conci et al., 2019), and acidic proteins
405 appear to evolve rapidly, species-specific proteins difficult to assign to cnidarian orthology groups
406 using similarity searches (Conci et al., 2020). Our results are consistent with that observation, as the
407 two acidic proteins found do not show significant similarity to other proteins deposited in public
408 databases such as SwissProt, and even within Cnidaria, only matched proteins found in other
409 octocorals. Among the group of taxonomically widespread proteins, we found typical components of
410 animal basement membranes (Erickson & Couchman, 2000) with a broad distribution within Cnidaria
411 and generally within Metazoa. Indeed, three of the six most abundant proteins, namely agrin,
412 collagen, and osteonidogen, are glycoproteins involved in modulating cell-extracellular matrix
413 interactions (Erickson & Couchman, 2000). Among vertebrates, agrin participates in synaptogenesis

414 (Kröger & Schröder, 2002). Specifically, this protein coordinates the development of neuromuscular
415 junctions, stabilizing and aligning the pre- and postsynaptic apparatuses of neurons and muscle
416 fibers, respectively. It also triggers the differentiation of neuron growth cones into presynaptic
417 terminals capable of calcium-dependent neurotransmission (Kröger & Schröder, 2002; Ruegg &
418 Bixby, 1998). Its presence in the SOM of sclerites may imply a similar role in calcification, aligning the
419 sclerocytes around sclerite primordia and triggering membrane differentiation to allow for calcium
420 secretion into the calcifying space. In line with this reasoning, in addition to biomineralization-
421 related GO-terms, colonies exposed to low pH stress modulated transcripts enriched in GO-terms,
422 pointing to the active regulation of processes involving the localization of proteins to synapses. We
423 did not observe any apparent effect of the pH treatment on colony behavior that suggested colonies
424 could not react to mechanical stimuli. Thus, we propose interpreting the localization of proteins to
425 "synapses" in a biomineralization context as the localization of proteins to calcification sites, which,
426 given the presence of presynaptic proteins, appear to be related to some extent synapses. Although
427 speculative at this point, the analysis of single-cell transcriptomes of octocorals exposed to low pH
428 seawater can help disentangle this stress' effect on different octocorals cell types (e.g., neurons vs.
429 sclerocytes). In the case of osteonidogen, mammalian osteocytes and osteoclasts overexpress this
430 protein (Barshis et al., 2013; Ramos-Silva et al., 2013), suggesting a direct role in calcification in that
431 group and a possible involvement in calcification in octocorals.
432
433 To respond more rapidly to and survive episodes of environmental stress, resilient stony corals
434 constitutively upregulate components of the coral cell death and immune pathways and genes
435 involved in response to stress, like heat-shock proteins (Barshis et al., 2013). The concomitant
436 downregulation of genes involved in calcification observed during environmental stress in these
437 organisms (Barshis et al., 2013; Ramos-Silva et al., 2013) suggests that the transcriptional
438 frontloading of the stress response toolkit comes at the expense of the coral calcification machinery
439 and could lead to its collapse. Accordingly, calcification in colonies of *Siderastrea siderea* exposed to

ocean acidification and warming shows a parabolic response, driven mainly by the abrupt drop in calcification rates under more extreme environmental regimes (Inoue et al., 2013; Ruzicka et al., 2013). Our results revealed a similar response of *P. flava* to heat stress, indicating a degree of commonality in the transcriptomic response of stony and soft corals to heat stress. Whether the octocorals' reaction to heat stress is generally similar to that of stony corals remains to be investigated in a larger sample of octocoral species to assess the universality of the pathways modulated during environmental stress.

Despite the observed similarities in the transcriptional response of the stress toolkit of stony corals and octocorals exposed to heat stress, the calcification machinery of these two groups appear to react differently to adverse environmental conditions. Contrary to stony corals, our results indicate that *P. flava* can sustain the production of all the molecules necessary for the formation of new sclerites during stress events. In this regard, we detected only a mild effect of environmental stress on the calcification toolkit of *P. flava*, with heat stress affecting the expression of a galaxin and a carbonic anhydrase and seawater pH stress modulating the expression of osteonidogen and a prosaposin homolog. Galaxins, carbonic anhydrases, and osteonidogen are calcification-related genes in corals and other organisms, and mutations in human prosaposin cause Gaucher's disease, a disorder characterized by skeleton deterioration (Vaccaro et al., 2010). The reported linear decrease in octocoral calcification rates under reduced seawater pH (Gómez et al., 2015) is consistent with the hypothesis of a decoupling between the calcification and stress-response toolkits of octocorals, as it indicates that the observed decrease in calcification is mainly driven by the environment, not by a transcriptional response of the octocoral calcification machinery to the adverse conditions. Under long-term adverse conditions, decoupling the physiological response to stress from calcification may give octocorals a competitive advantage over other species, like stony corals, adapted to respond better to episodic stress and lead to the community shifts observed in many reef locations (Inoue et al., 2013a; Ruzicka et al., 2013). Characterizing the transcriptional response to environmental stress

of a broader taxonomic sample of octocorals will determine whether the calcification toolkit of these organisms is transcriptionally resilient.

In summary, our results provide new insights into the octocoral stress response to environmental stress. They suggest that the calcification and the stress-response toolkits of soft and stony corals react differently to stress episodes. This difference likely determines the somewhat contrasting response to stress observed in these groups. Anthropogenic-induced global climate change will undoubtedly impact future marine communities in unprecedented ways (Hughes et al., 2019). Processes such as acclimatization and adaptation (Palumbi, Barshis, Traylor-Knowles, & Bay, 2014), acting at organismal and population levels, and phenomena affecting the community, like ecological memory (Hughes et al., 2019), shape the response of coral reefs to these environmental pressures. Our results suggest that, compared to stony corals, octocorals use different gene regulation strategies to face climate change. Thus, understanding the diversity of molecular mechanisms involved in resilience and their regulation in different reef organisms is pivotal to predicting the future of the world's coral reefs.

Acknowledgments

We thank Gabriele Büttner for support during laboratory work and Dr. Peter Naumann for supporting the aquarium facilities of the Section of Geobiology and Paleobiology of the Dept. of Earth & Environmental Sciences. We would also like to thank René Neumaier for our High-Performance Computing system's design, administration, and support; our work would be impossible without his careful and detailed work. The Deutsche Forschungs Gesellschaft funded this study through the grants Va1146-2/1 and Wo896-18/1. GW acknowledges funding through the LMU Munich's Institutional Strategy LMUexcellent within the framework of the German Excellence Initiative. SV thanks N. Villalobos T., M. Vargas V., S. Vargas V. and S. Vargas V. for their support.

References

Alexa, A., & Rahnenfuhrer, J. (2016). *topGO: Enrichment Analysis for Gene Ontology* [R Package version 2.30.1].

Atrigenio, M., Aliño, P., & Conaco, C. (2017). Influence of the Blue Coral *Heliopora coerulea* on Scleractinian Coral Larval Recruitment. *Journal of Marine Biology*, *2017*. doi: 10.1155/2017/6015143

Barshis, D. J., Ladner, J. T., Oliver, T. A., Seneca, F. O., Traylor-Knowles, N., & Palumbi, S. R. (2013). Genomic basis for coral resilience to climate change. *Proceedings of the National Academy of Sciences of the United States of America*, *110*(4), 1387–1392.

Bechtel, M., Keller, M. V., Bloch, W., Sasaki, T., Boukamp, P., Zaucke, F., … Nischt, R. (2012). Different domains in nidogen-1 and nidogen-2 drive basement membrane formation in skin organotypic cocultures. *FASEB Journal: Official Publication of the Federation of American Societies for Experimental Biology*, *26*(9), 3637–3648.

Buhl-Mortensen, L., & Mortensen, P. B. (2005). Distribution and diversity of species associated with deep-sea gorgonian corals off Atlantic Canada. In A. Freiwald & J. M. Roberts (Eds.), *Cold-Water Corals and Ecosystems* (pp. 849–879). Berlin, Heidelberg: Springer Berlin Heidelberg.

Castillo, K. D., Ries, J. B., Bruno, J. F., & Westfield, I. T. (2014). The reef-building coral *Siderastrea siderea* exhibits parabolic responses to ocean acidification and warming. *Proceedings of the Royal Society B*, *281*(1797). doi: 10.1098/rspb.2014.1856

Colgan, M. W. (1984). The Cretaceous Coral Heliopora (Octocorallia, Coenothecalia)—a Common Indo-Pacific Reef Builder. In N. Eldredge & S. M. Stanley (Eds.), *Living Fossils* (pp. 266–271). New York, NY: Springer New York.

Conci, N., Lehmann, M., Vargas, S., & Wörheide, G. (2020). Comparative Proteomics of Octocoral and Scleractinian Skeletomes and the Evolution of Coral Calcification. *Genome Biology and Evolution*, *12*(9), 1623–1635.

Conci, N., Wörheide, G., & Vargas, S. (2019). New Non-Bilaterian Transcriptomes Provide Novel Insights into the Evolution of Coral Skeletomes. *Genome Biology and Evolution*, *11*(11), 3068–3081.

Cox, J., Hein, M. Y., Luber, C. A., Paron, I., Nagaraj, N., & Mann, M. (2014). Accurate proteome-wide label-free quantification by delayed normalization and maximal peptide ratio extraction, termed MaxLFQ. *Molecular & Cellular Proteomics: MCP*, *13*(9), 2513–2526.

Cúrdia, J., Carvalho, S., Pereira, F., Guerra-García, J. M., Santos, M. N., & Cunha, M. R. (2015). Diversity and abundance of invertebrate epifaunal assemblages associated with gorgonians are driven by colony attributes. *Coral Reefs* , *34*(2), 611–624.

Davies, S. W., Marchetti, A., Ries, J. B., & Castillo, K. D. (2016). Thermal and pCO2 Stress Elicit Divergent Transcriptomic Responses in a Resilient Coral. *Frontiers in Marine Science*, *3*, 112.

Dixon, G., Abbott, E., & Matz, M. (2020). Meta-analysis of the coral environmental stress response: *Acropora* corals show opposing responses depending on stress intensity. *Molecular Ecology*, *29*(15), 2855–2870.

Done, T. J. (1992). Phase shifts in coral reef communities and their ecological significance. *Hydrobiologia*, *247*(1), 121–132.

Drake, J. L., Mass, T., Haramaty, L., Zelzion, E., Bhattacharya, D., & Falkowski, P. G. (2013). Proteomic analysis of skeletal organic matrix from the stony coral *Stylophora pistillata* . *Proceedings of the National Academy of Sciences of the United States of America*, *110*(10), 3788–3793.

Eitel, M., Francis, W. R., Varoqueaux, F., Daraspe, J., Osigus, H.-J., Krebs, S., … Wörheide, G. (2018). Comparative genomics and the nature of placozoan species. *PLoS Biology*, *16*(7), e2005359.

Erickson, A. C., & Couchman, J. R. (2000). Still more complexity in mammalian basement membranes. *The Journal of Histochemistry and Cytochemistry: Official Journal of the Histochemistry Society*, *48*(10), 1291–1306.

Fung, T., Seymour, R. M., & Johnson, C. R. (2011). Alternative stable states and phase shifts in coral reefs under anthropogenic stress. *Ecology*, *92*(4), 967–982.

Gabay, Y., Benayahu, Y., & Fine, M. (2013). Does elevated pCO2 affect reef octocorals? *Ecology and Evolution*, *3*(3), 465–473.

Gabay, Y., Fine, M., Barkay, Z., & Benayahu, Y. (2014). Octocoral tissue provides protection from declining oceanic pH. *PloS One*, *9*(4), e91553.

Goldberg, W. M., & Benayahu, Y. (1987). Spicule formation in the gorgonian coral *Pseudoplexaura flagellosa*. 1: Demonstration of intracellular and extracellular growth and the effect of ruthenium red during decalcification. *Bulletin of Marine Science*, *40*(2), 287–303.

Gómez, C. E., Paul, V. J., Ritson-Williams, R., Muehllehner, N., Langdon, C., & Sánchez, J. A. (2015). Responses of the tropical gorgonian coral *Eunicea fusca* to ocean acidification conditions. *Coral Reefs* , *34*(2), 451–460.

González-Pech, R. A., Vargas, S., Francis, W. R., & Wörheide, G. (2017). Transcriptomic Resilience of the *Montipora digitata* Holobiont to Low pH. *Frontiers in Marine Science*, *4*, 403.

Holcomb, M., Cohen, A. L., & McCorkle, D. C. (2013/2). An evaluation of staining techniques for marking daily growth in scleractinian corals. *Journal of Experimental Marine Biology and Ecology*, *440*, 126–131.

Howison, M., Sinnott-Armstrong, N. A., & Dunn, C. W. (2012). BioLite, a Lightweight Bioinformatics Framework with Automated Tracking of Diagnostics and Provenance. *TaPP*. Retrieved from https://www.usenix.org/system/files/conference/tapp12/tapp12-final5.pdf

Hughes, T. P., Barnes, M. L., Bellwood, D. R., Cinner, J. E., Cumming, G. S., Jackson, J. B. C., … Scheffer, M. (2017). Coral reefs in the Anthropocene. *Nature*, *546*(7656), 82–90.

Hughes, T. P., Kerry, J. T., Baird, A. H., Connolly, S. R., Dietzel, A., Eakin, C. M., … Torda, G. (2018). Global warming transforms coral reef assemblages. *Nature*, *556*(7702), 492–496.

Hughes, T. P., Kerry, J. T., Connolly, S. R., Baird, A. H., Eakin, C. M., Heron, S. F., … Torda, G. (2019). Ecological memory modifies the cumulative impact of recurrent climate extremes. *Nature Climate Change*, *9*(1), 40–43.

Inoue, S., Kayanne, H., Yamamoto, S., & Kurihara, H. (2013). Spatial community shift from hard to soft corals in acidified water. *Nature Climate Change*, *3*(7), 683–687.

Kayanne, H., Harii, S., Ide, Y., & Akimoto, F. (2002). Recovery of coral populations after the 1998 bleaching on Shiraho Reef, in the southern Ryukyus, NW Pacific. *Marine Ecology Progress Series*, Vol. 239, pp. 93–103. doi: 10.3354/meps239093

Kingsley, R. J. (1984). Spicule Formation in the Invertebrates with Special Reference to the Gorgonian *Leptogorgia virgulata*. *Integrative and Comparative Biology*, *24*(4), 883–891.

Kingsley, R. J., & Watabe, N. (1989). The dynamics of spicule calcification in whole colonies of the gorgonian *Leptogorgia virgulata* (Lamarck) (Coelenterata: Gorgonacea). *Journal of Experimental Marine Biology and Ecology*, *133*(1), 57–65.

Kröger, S., & Schröder, J. E. (2002). Agrin in the developing CNS: new roles for a synapse organizer. *News in Physiological Sciences: An International Journal of Physiology Produced Jointly by the International Union of Physiological Sciences and the American Physiological Society*, *17*, 207–212.

Lewis, J. C., & Vonwallis, E. (1991). THE FUNCTION OF SURFACE SCLERITES IN GORGONIANS (COELENTERATA, OCTOCORALLIA). *The Biological Bulletin*, *181*(2), 275–288.

Lopes, A. R., Faleiro, F., Rosa, I. C., Pimentel, M. S., Trubenbach, K., Repolho, T., … Rosa, R. (2018). Physiological resilience of a temperate soft coral to ocean warming and acidification. *Cell Stress & Chaperones*, *23*(5), 1093–1100.

Love, M. I., Huber, W., & Anders, S. (2014). Moderated estimation of fold change and dispersion for RNA-seq data with DESeq2. *Genome Biology*, *15*(12), 550.

Moya, A., Huisman, L., Ball, E. E., Hayward, D. C., Grasso, L. C., Chua, C. M., … Miller, D. J. (2012). Whole transcriptome analysis of the coral *Acropora millepora* reveals complex responses to CO2-driven acidification during the initiation of calcification. *Molecular Ecology*, *21*(10), 2440–2454.

Norström, A. V., Nyström, M., Lokrantz, J., & Folke, C. (2009). Alternative states on coral reefs: beyond coral–macroalgal phase shifts. *Marine Ecology Progress Series*, *376*, 295–306.

Palumbi, S. R., Barshis, D. J., Traylor-Knowles, N., & Bay, R. A. (2014). Mechanisms of reef coral resistance to future climate change. *Science*, *344*(6186), 895–898.

Patro, R., Duggal, G., Love, M. I., Irizarry, R. A., & Kingsford, C. (2017). Salmon provides fast and bias-aware quantification of transcript expression. *Nature Methods*, *14*(4), 417–419.

Petersen, T. N., Brunak, S., von Heijne, G., & Nielsen, H. (2011). SignalP 4.0: discriminating signal peptides from transmembrane regions. *Nature Methods*, *8*(10), 785–786.

Quattrini, A. M., Etnoyer, P. J., Doughty, C., English, L., Falco, R., Remon, N., … Cordes, E. E. (2014). A phylogenetic approach to octocoral community structure in the deep Gulf of Mexico. *Deep-Sea Research. Part II, Topical Studies in Oceanography*, *99*, 92–102.

Ramos-Silva, P., Kaandorp, J., Huisman, L., Marie, B., Zanella-Cléon, I., Guichard, N., … Marin, F. (2013). The skeletal proteome of the coral *Acropora millepora*: the evolution of calcification by co-option and domain shuffling. *Molecular Biology and Evolution*, *30*(9), 2099–2112.

Ruegg, M. A., & Bixby, J. L. (1998). Agrin orchestrates synaptic differentiation at the vertebrate neuromuscular junction. *Trends in Neurosciences*, *21*(1), 22–27.

Ruzicka, R. R., Colella, M. A., Porter, J. W., Morrison, J. M., Kidney, J. A., Brinkhuis, V., … Colee, J. (2013). Temporal changes in benthic assemblages on Florida Keys reefs 11 years after the 1997/1998 El Niño. *Marine Ecology Progress Series*, *489*, 125–141.

Schmitt, R. J., Holbrook, S. J., Davis, S. L., Brooks, A. J., & Adam, T. C. (2019). Experimental support for alternative attractors on coral reefs. *Proceedings of the National Academy of Sciences of the United States of America*, *116*(10), 4372–4381.

Schwanhäusser, B., Busse, D., Li, N., Dittmar, G., Schuchhardt, J., Wolf, J., … Selbach, M. (2011). Global quantification of mammalian gene expression control. *Nature*, *473*(7347), 337–342.

Seneca, F. O., & Palumbi, S. R. (2015). The role of transcriptome resilience in resistance of corals to bleaching. *Molecular Ecology*, *24*(7), 1467–1484.

Shaish, L., Levy, G., Katzir, G., & Rinkevich, B. (2010). Coral Reef Restoration (Bolinao, Philippines) in the Face of Frequent Natural Catastrophes. *Restoration Ecology*, *18*(3), 285–299.

Shimpi, G. G., Vargas, S., & Wörheide, G. (2016). Evaluation and validation of reference genes for qPCR analysis to study climate change-induced stresses in *Sinularia* cf. *cruciata* (Octocorallia: Alcyonidae). *Journal of Experimental Marine Biology and Ecology*, *483*, 42–52.

Spencer, T., Laughton, A. S., Flemming, N. C., Stobart, B., Teleki, K., Buckley, R., … Callow, M. (2005). Coral recovery at Aldabra Atoll, Seychelles: five years after the 1998 bleaching event. *Philosophical Transactions of the Royal Society A: Mathematical, Physical and Engineering Sciences*, *363*(1826), 251–255.

Thomas, L., Rose, N. H., Bay, R. A., López, E. H., Morikawa, M. K., Ruiz-Jones, L., & Palumbi, S. R. (2018). Mechanisms of Thermal Tolerance in Reef-Building Corals across a Fine-Grained Environmental Mosaic: Lessons from Ofu, American Samoa. *Frontiers in Marine Science*, *4*, 434.

Vaccaro, A. M., Motta, M., Tatti, M., Scarpa, S., Masuelli, L., Bhat, M., … Salvioli, R. (2010). Saposin C mutations in Gaucher disease patients resulting in lysosomal lipid accumulation, saposin C deficiency, but normal prosaposin processing and sorting. *Human Molecular Genetics*, *19*(15), 2987–2997.

Wessel, D., & Flügge, U. I. (1984). A method for the quantitative recovery of protein in dilute solution in the presence of detergents and lipids. *Analytical Biochemistry*, *138*(1), 141–143.

Wiens, M., Ammar, M. S., Nawar, A. H., Koziol, C., Hassanein, H. M., Eisinger, M., … Müller, W. E. (2000). Induction of heat-shock (stress) protein gene expression by selected natural and

anthropogenic disturbances in the octocoral *Dendronephthya klunzingeri*. *Journal of Experimental Marine Biology and Ecology*, *245*(2), 265–276.

Yu, G., Li, F., Qin, Y., Bo, X., Wu, Y., & Wang, S. (2010). GOSemSim: an R package for measuring semantic similarity among GO terms and gene products. *Bioinformatics* , *26*(7), 976–978.

Data availability statement:

- Raw sequence reads: European Nucleotide Archive project PRJEB38757, accession numbers ERS4652944-ERS4652972.
- Raw MS/MS data files: https://data.ub.uni-muenchen.de/189/
- Transcriptome assembly, proteome annotations, count matrix, scripts, and other data files used in this study: https://gitlab.lrz.de/palmuc/pinnigorgia_resilience

Author Contributions:

SV Conceptualization, Methodology, Software, Validation, Formal Analysis, Investigation, Resources, Data Curation, Writing - Original Draft, Visualization, Supervision, Funding Acquisition. **TZ** Investigation, Formal Analysis. **NC** Investigation, Formal Analysis, Writing - Review & Editing. **ML** Investigation. **GW** Resources, Writing - Review & Editing, Funding Acquisition.

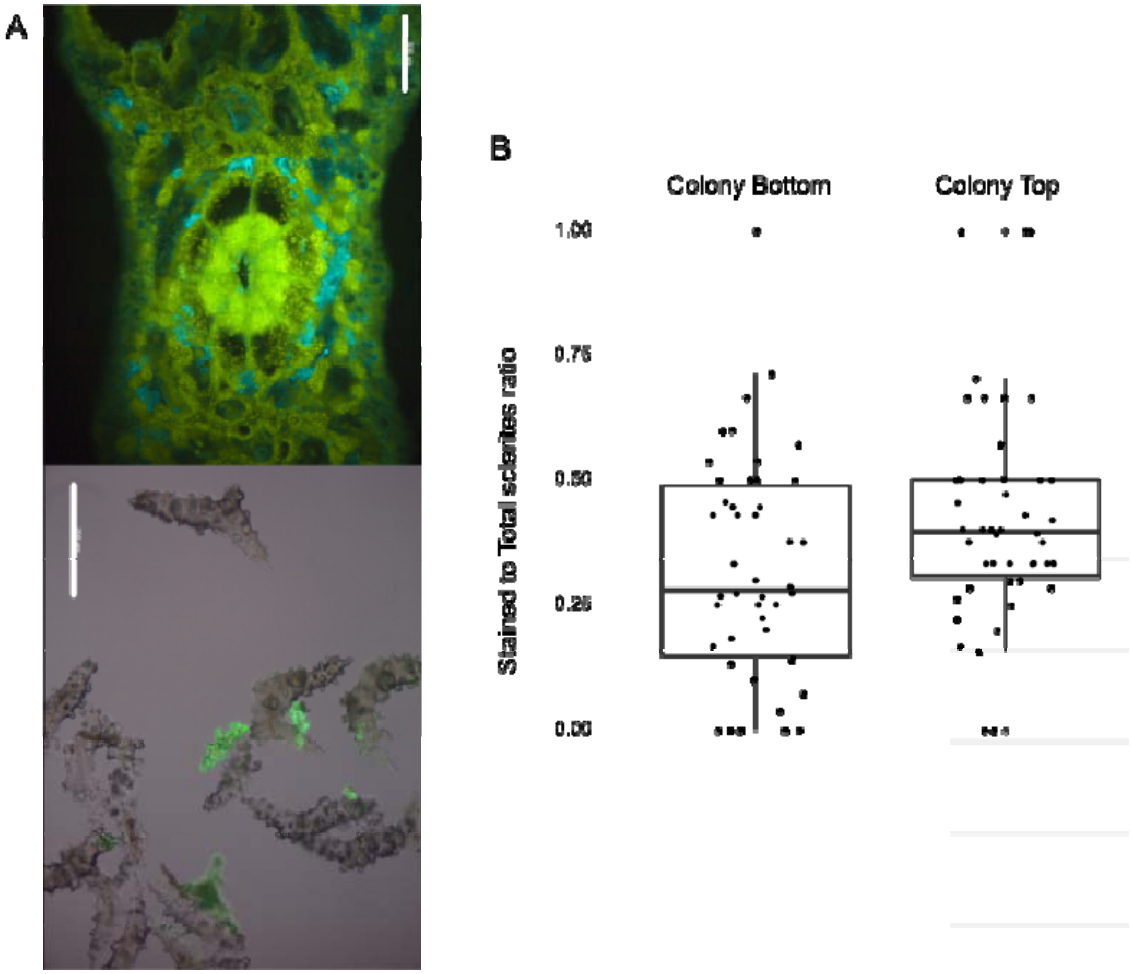

Figure 1. Calcification in *Pinnigorgia flava*. **A:** *In situ* (blue hue used to differentiate calcein staining from tissue autofluorescence) and isolated calcein-stained sclerites (green fluorescent), note the distribution of newly deposited $CaCO_3$ (lighter green dots) around the polyp (figure center). Both scale bars = 200µm. **B:** ratio of calcein-stained to total number of sclerites in bottom vs. top colony parts. Welch two-sample t=-2.17, df=92.531, p=0.034.

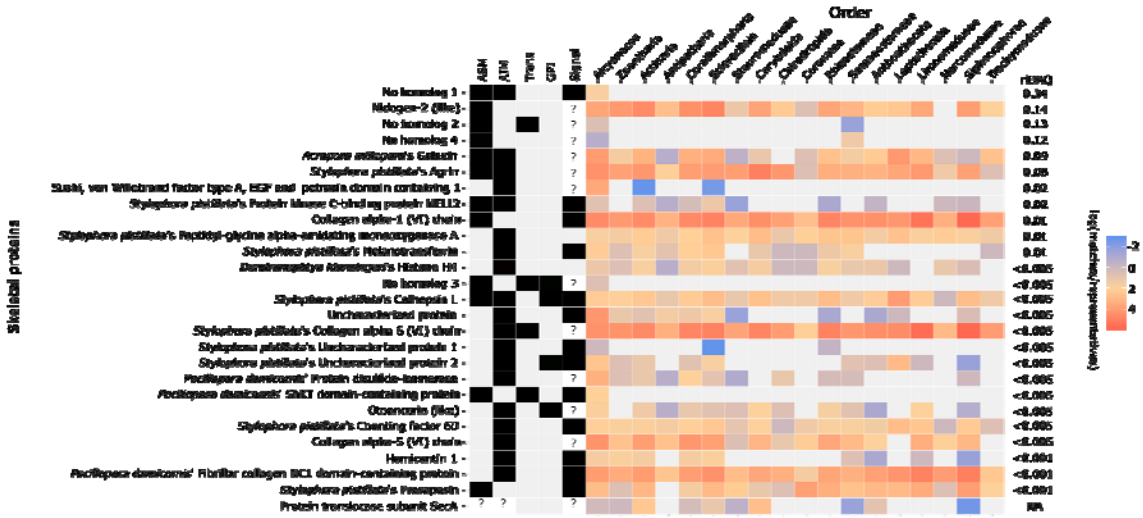

Figure 2. Presence/absence (black/gray rectangles, respectively) in the acid-soluble (ASM) and insoluble (AIM) matrix, biochemical properties, distribution among cnidarians, and abundance in the skeletal proteome of 27 proteins present in the skeleton of *P. flava*. Trans: Presence of transmembrane domains. GPI: Presence of GPI anchors. Signal: Presence of signal peptide.A question mark (?) indicates that the particular property could not be determined, e.g., due to the availability of only partial sequences.

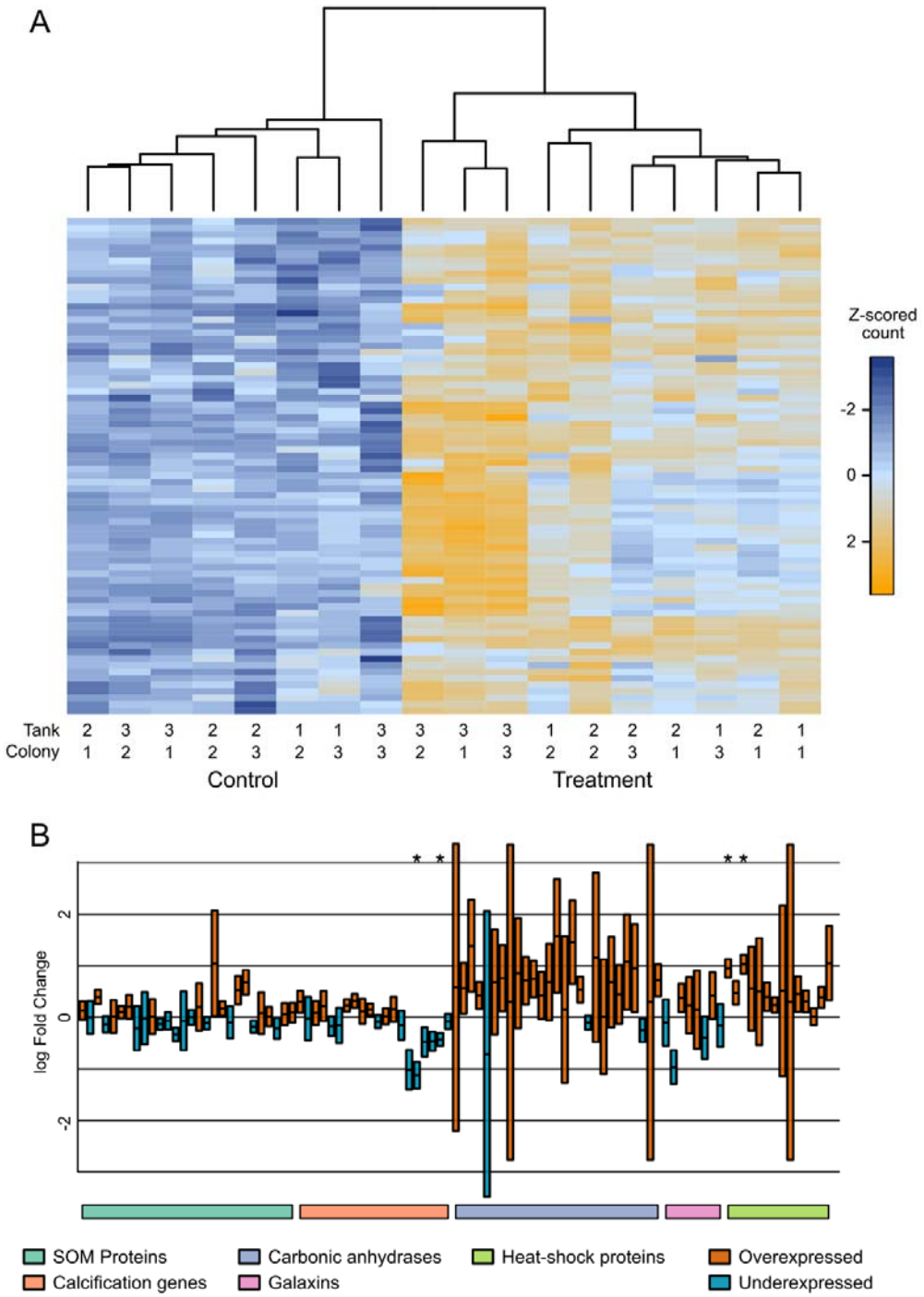

Figure 3. A: Expression (variance stabilized, z-scored transformed counts) of 76 transcripts modulated in *P.flava* colonies exposed to control and heat stress. For visualization purposes only transcripts with log2 fold change ≥ |1| and $p < 0.01$ were included in the heat plot. **B:** Change in gene expression of 27 SOM proteins, calcification related proteins *sensu* Conci et al. (2019), carbonic anhydrases, galaxins, and heat-shock proteins in *P. flava* colonies exposed to heat stress. The asterisks (*) indicate transcripts significantly differentially expressed in control vs. treatment samples.

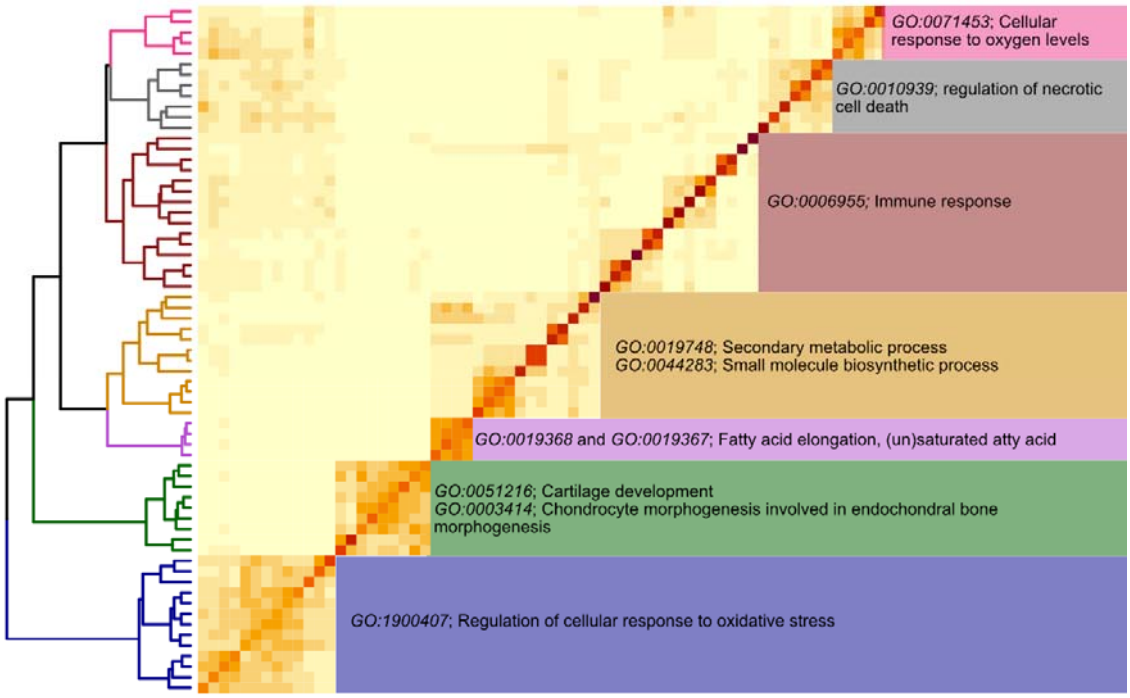

Figure 4. Clusters of semantically similar, significantly enriched Biological Process GO-terms found in the set of overexpressed genes under heat stress. Characteristic GO-terms are annotated to the right of each cluster.

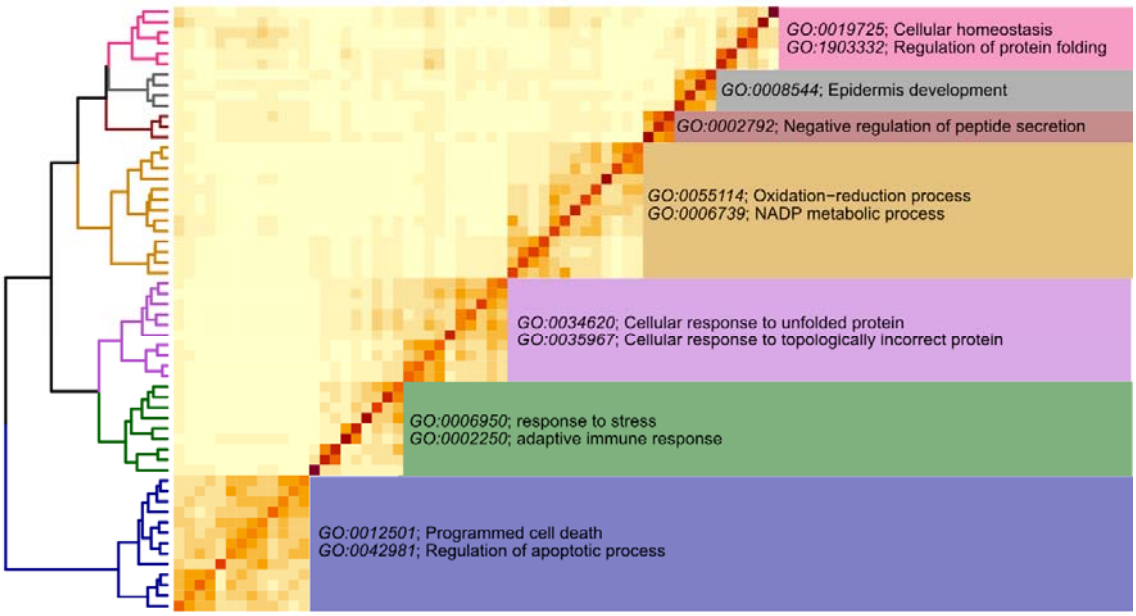

Figure 5. Clusters of semantically similar, significantly enriched Biological Process GO-terms found in the set of underexpressed genes under heat stress. Characteristic GO-terms are annotated to the right of each cluster.

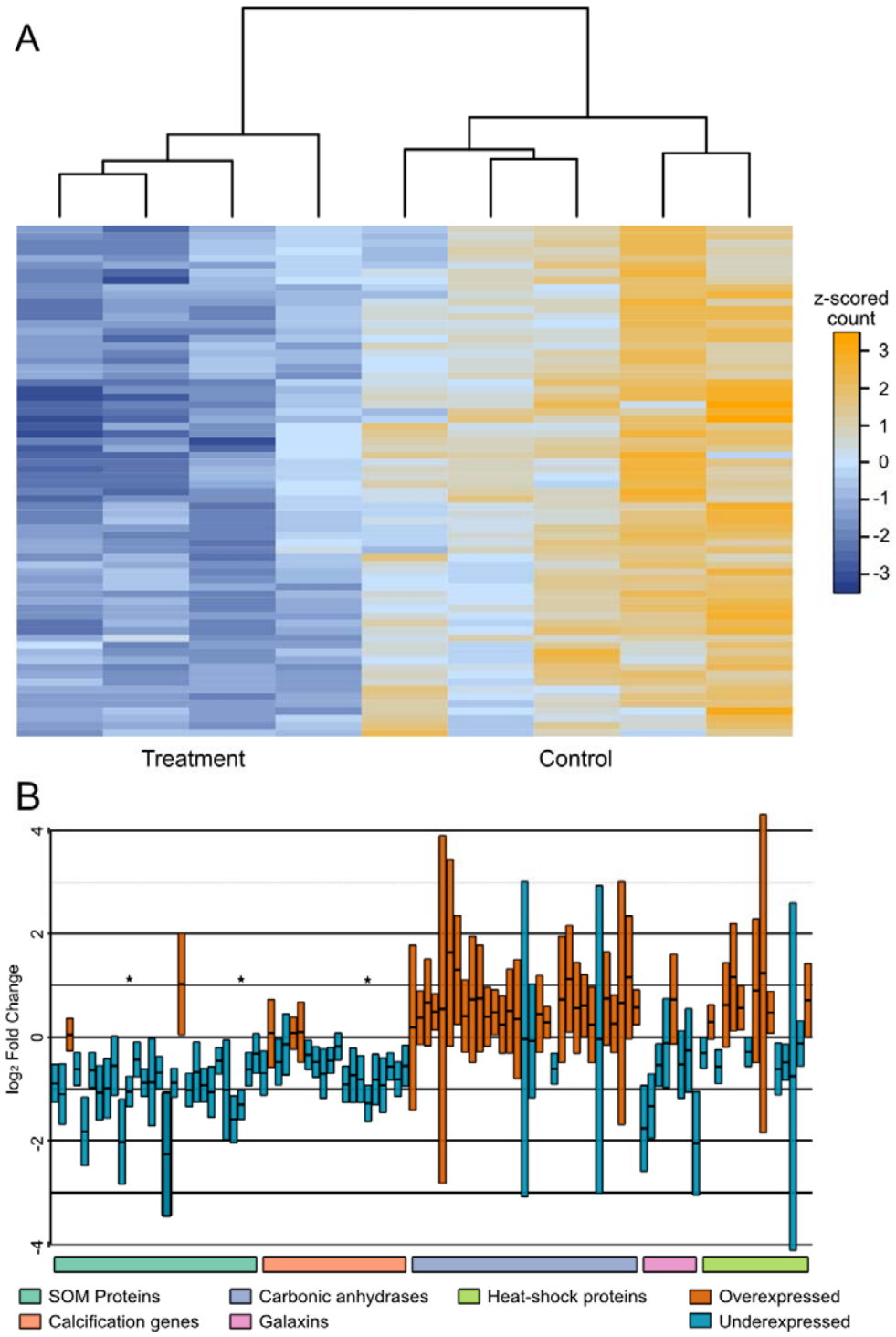

Figure 6 . A: Expression (variance stabilized, z-scored transformed counts) of 70 transcripts modulated ($p < 0.05$) in *P.flava* colonies exposed to control and low pH stress. **B:** Change in gene expression of 27 SOM proteins, calcification related proteins *sensu* Conci et al. (2019), carbonic anhydrases, galaxins, and heat-shock proteins in *P. flava* colonies exposed to low pH stress. The asterisks (*) indicate transcripts significantly differentially expressed in control vs. treatment samples.

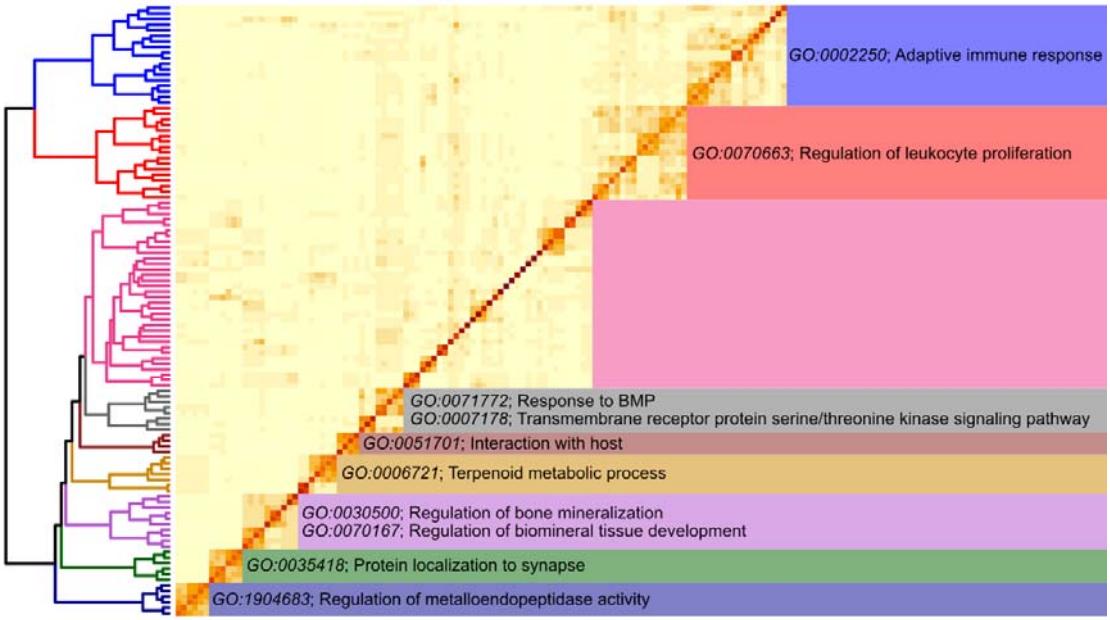

Figure 7. Clusters of semantically similar, significantly enriched Biological Process GO-terms found in the set of underexpressed genes under pH stress. Characteristic GO-terms are annotated to the right of each cluster.